IL-6 modulates the immune status of the tumor microenvironment to facilitate metastatic colonization of colorectal cancer cells

Yujiro Toyoshima[1,2], Hidemitsu Kitamura[1*], Huihui Xiang[1,2], Yosuke Ohno[2], Shigenori Homma[2], Hideki Kawamura[2], Norihiko Takahashi[2], Toshiya Kamiyama[2], Mishie Tanino[3], Akinobu Taketomi[2]

[1]Division of Functional Immunology, Section of Disease Control, Institute for Genetic Medicine, Hokkaido University, Sapporo 06-0815, Japan

[2]Department of Gastroenterological Surgery I, Hokkaido University Graduate School of Medicine, Sapporo 060-8638, Japan

[3]Department of Surgical Pathology, Asahikawa Medical University, Asahikawa 078-8510, Japan.

Running Title: IL-6 facilitates metastatic colonization of colon cancer

Keywords: IL-6, metastatic colonization, colorectal cancer, dendritic cells, killer T cells

Additional information:

This work was partially supported by Grants-in-Aid for Scientific Research (C) (25460584 to H. Kitamura and 16K10526 to N. Takahashi) from the Japan Society for the Promotion of Science (JSPS), the Platform Project for Supporting Drug Discovery and Life Science Research (Platform for Drug Discovery, Informatics, and Structural Life Science) from the Ministry of Education, Culture, Sports, Science and Technology (MEXT) of Japan (to H. Kitamura), the Japan Agency for Medical Research and Development (AMED) (to A. Taketomi), and the Joint Research Program of the Institute for Genetic Medicine, Hokkaido University (to M. Tanino and A. Taketomi).

*__Address correspondence and reprint requests to__ Dr. Hidemitsu Kitamura,

Division of Functional Immunology, Section of Disease Control, Institute for Genetic Medicine, Hokkaido University, Kita-15, Nishi-7, Kita-ku, Sapporo 060-0815, Japan

Tel: +81-11-706-5520, Fax: +81-11-706-5519

E-mail: kitamura@igm.hokudai.ac.jp

No potential conflicts of interest were disclosed.

Word count in the main text : 5913 words (including 6 figures, 2 supplementary tables and 9 supplementary figures)

Abstract

It is unknown as to how liver metastases are correlated with host immune status in colorectal cancer. In this study, we found that IL-6, a proinflammatory cytokine produced in tumor-bearing states, promotes the metastatic colonization of colon cancer cells in association with dysfunctional anti-tumor immunity. In IL-6-deficient mice, metastatic colonization of CT26 cells in the liver was reduced, and the anti-tumor effector function of $CD8^+$ T cells as well as IL-12 production by $CD11c^+$ dendritic cells were augmented *in vivo*. Furthermore, IL-6-deficient mice exhibited enhanced IFN-AR1-mediated type I interferon signaling, which upregulated PD-L1 and MHC class I expression on CT26 cells. *In vivo* injection of anti-PD-L1 antibody effectively suppressed the metastatic colonization of CT26 cells in *Il6*$^{-/-}$ but not *Il6*$^{+/+}$ mice. Finally, we confirmed that colorectal cancer patients with low IL-6 levels in their primary tumors showed prolonged disease-free survival. These findings suggest IL-6 may be a promising target for the treatment of metastasis in colorectal cancers by improving host immunity.

Introduction

The suppression of anti-tumor effector cells in a tumor-bearing host is a critical problem for the immunotherapy of cancer patients. Immune checkpoint inhibitors such as anti-CTLA4, anti-PD-1, and PD-L1 antibodies have enabled curative treatment for some advanced cancers (1, 2). However, the clinical efficacy of immune checkpoint blockade therapy for cancer varies according to the tumor type and between individual patients, suggesting that several different immunosuppressive mechanisms might operate in tumor-bearing hosts (3, 4). Therefore, alternative or additional targets to improve host immune status are required for the development of cancer immunotherapy with improved effectiveness.

Interleukin-6 (IL-6), a multipotent cytokine, binds to IL-6 receptor alpha (IL-6Ra) expressed on target cells. IL-6/IL-6Ra complexes with gp130, a signal transducer, to recruit Janus kinase, which phosphorylates signal transducer and activator of transcription 3 (STAT3). Phosphorylated STAT3 translocates to the nucleus and induces the transcription of various target genes to regulate cellular functions such as the proliferation, survival and differentiation of various cell types including epithelial cells, endothelial cells, fibroblasts, osteocytes, immune cells, and cancer cells (5-7).

We previously demonstrated that activation of the IL-6/STAT3 signaling cascade in dendritic cells (DCs) caused a reduction in antigen presentation ability and

suppressed the subsequent antigen-specific helper and killer T cell responses *in vitro* and *in vivo* (8, 9). Furthermore, we revealed that blockade of IL-6 signaling through the administration of anti-IL-6Ra monoclonal antibody (mAb) to tumor-bearing mice significantly inhibited tumor growth by enhancing the effector function of $CD8^+$ T cells (10, 11).

Recently, we demonstrated that IL-6 inhibits the maturation and antigen presentation of human monocyte-derived DCs and suppresses antigen-specific T cell responses in an IL-12-dependent manner (12). In this study, *IL6* gene expression was higher in $CD11b^+CD11c^+$ cells in the tumor tissues of colorectal cancer (CRC) patients compared with peripheral blood mononuclear cells (PBMCs). This confirmed that the TCR-mediated activation of both $CD4^+$ T cells and $CD8^+$ T cells was significantly reduced in the presence of $CD11b^+CD11c^+$ cells in tumor tissues compared with PBMCs.

CRC, a leading cause of mortality, is the second most common cancer in women and the third most common cancer in men worldwide. It was reported that approximately 694,000 individuals died of CRC in 2012 (13, 14). Metastasis is one of the most severe risk factors for cancer death, and the liver is the most frequent site for the metastasis of colon cancer cells; however, the precise mechanism of liver metastasis with regards to the host's immune system has not been fully elucidated (15,

16). Identification of the causes of liver metastasis might therefore be a critical step towards controlling CRC. This study aimed to elucidate the precise mechanisms involved in the regulation of liver metastasis and how they correlate to host immunity.

We investigated whether IL-6 is related to the metastatic colonization of colon cancer cells by inhibiting anti-tumor immunity in mouse models. We report that IL-6 produced by tumor-bearing hosts contributed to the progress of metastatic colonization of colon cancer cells through the suppression of anti-tumor effector cells including $CD8^+$ T cells.

Materials and methods

Mice and cells

Wild-type BALB/c (*Il6*$^{+/+}$) mice were obtained from Charles River Japan (Kanagawa, Japan). BALB/c background IL-6-deficient (*Il6*$^{-/-}$) mice were obtained from the Center for Animal Disease Models, Research Institute for Biomedical Sciences, Tokyo University of Science (Chiba, Japan). All mice were maintained in specific pathogen-free conditions in accordance with the guidelines of the Animal Department at Hokkaido University and were used at 6–8 weeks of age. The murine colon cancer cell line CT26 (CRL-2638) and murine breast cancer cell line 4T1 (CRL-2539) were obtained from the American Type Culture Collection (Manassas, VA, USA). All mouse experiments were approved by the Animal Ethics Committee of Hokkaido University (No. 14-0062) and conducted in accordance with the recommendations of the Guide for the Care and Use of Laboratory Animals of the University, an Institutional Animal Care and Use Committee.

Human subjects

Research protocols involving human subjects were approved by the institutional review board of Hokkaido University Graduate School of Medicine (14-043) and the Institute for Genetic Medicine (14-005, 14-0004). Written informed consent was obtained from

each patient. In total, 108 CRC patients who underwent surgery at Hokkaido University Hospital between 2003 and 2015 were included in this study. Patients were followed up at 1–6-month intervals until death or until 31 March 2019. Patient clinical features are shown in Supplementary Table S1.

Antibodies and reagents

The following monoclonal antibodies (mAb) were obtained from BioLegend (San Diego, CA, USA) or BD Biosciences (San Diego, CA, USA): fluorescent dye-conjugated anti-CD45 (30-F11), APC-conjugated anti-mouse CD11c (N418), APC-conjugated CD4 (RM4-5), APC-Cy7-conjugated anti-mouse CD8a (53-6.7), FITC-conjugated CD44 (IM7), PE-conjugated anti-mouse CD62L (MEL-14), anti-H-2K^{d} (AF6-88.5), anti-I-A^{d} (AF6-120.1), and APC-conjugated anti-mouse CD274 (10F.9G2). PE-conjugated anti-mouse perforin (eBioOMAK-D) and PE-conjugated anti-mouse granzyme B (NGZB) were obtained from eBioscience (Tokyo, Japan). 7-AAD Viability Dye was purchased from Beckman Coulter (Marseille Cedex, France). mAbs for IL-6 neutralization (clone MP5-20F3), CD8 depletion (clone 53.6.7), IL-12 neutralization (clone C17.8), IFN-AR1 signaling inhibition (clone MAR1-5A3), and an antagonist mAb against PD-L1 (clone 10F.9G2) were purchased from Bio X Cell (West Lebanon, NH, USA). Clophosome-clodronate liposomes and control liposomes (Neutrl) (F70101-N) were purchased from

FormuMax (Sunnyvale, CA, USA). Recombinant murine IFN-α (752802) was purchased from BioLegend. Recombinant murine IFN-β was purchased from PeproTech EC Ltd. (Hammersmith, London, UK). Phorbol 12-myristate 13-acetate (PMA) and A23187 calcium ionophore were purchased from Sigma-Aldrich (St. Louis, MO, USA).

Cell culture

CT26 cells were maintained in RPMI-1640 medium (Wako Pure Chemical Industries, Ltd., Osaka, Japan) supplemented with 10% fetal bovine serum, 200 U/ml penicillin, 100 μg/ml streptomycin, 10 mM HEPES, and 0.05 mmol/L 2-mercaptoethanol (Sigma-Aldrich, Tokyo, Japan) at 37°C in a humidified atmosphere containing 5% CO_2. For flow cytometry, CT26 cells (2.5×10^5) were cultured in 12-well culture plates and treated with IFN-α or IFN-β (50 ng/mL) in the presence or absence of STAT1 inhibitor (2 μg/mL) for 24 h.

Metastatic colonization model

GFP-transfected CT26 cells (2×10^5) were inoculated intrasplenically (i.s.) or intravenously (i.v.) into *Il6*$^{+/+}$ or *Il6*$^{-/-}$ BALB/c mice. Metastatic colonization images of CT26-GFP-positive tumors in liver or lung tissue were evaluated using an *in vivo*

imaging system (IVIS Spectrum, Xenogen) at day 14. For *ex vivo* analysis, CT26 cells were transfected with pMX-IRES-GFP, obtained from Dr. T. Kitamura (The University of Tokyo), using Lipofectamine 3000 (Thermo Fisher Scientific, Waltham, Massachusetts, USA). These GFP-transduced CT26 cells were used in the tumor-bearing mouse models. Anti-CD8 mAb and other mAbs or control IgG (200 μg/mouse) were injected intraperitoneally into *Il6*$^{+/+}$ and *Il6*$^{-/-}$ mice at days −1 and +5, and then every 4 days thereafter. Anti-PD-L1 mAb (200 μg/mouse) or control IgG (200 μg/mouse) were i.p. injected into CT26 tumor-bearing *Il6*$^{+/+}$ and *Il6*$^{-/-}$ mice at day 5 and then every 4 days thereafter. Livers were excised from mice, and after collagenase treatment and homogenization, mononuclear cells were isolated from whole liver cells by centrifugation using Percoll. Population analysis and cytotoxicity assays were performed by flow cytometry.

ELISA

We determined IL-6 levels in serum obtained from CT26-inoculated *Il6*$^{+/+}$ and *Il6*$^{-/-}$ mice at day 14 and normal mice using an OptEIA Mouse IL-6 ELISA Kit (BD Biosciences) according to the manufacturer's instructions.

PCR analysis

Total RNA was extracted from murine 7AAD^{-}CD45^{+}CD11c^{+} cells and whole cells derived from liver metastatic tissues using ISOGEN (Nippon Gene, Toyama, Japan) in accordance with the manufacturer's instructions. First-strand cDNA was synthesized using 1 μg of total RNA, oligo (dT) (Invitrogen, Carlsbad, CA), and Superscript III reverse transcriptase (Invitrogen**,** Carlsbad, CA). Genes encoding murine *Ifna, Ifnb, Il12a, Il12b, Arg1, Il10*, and *Actb* were amplified using a Real-time PCR Detection System (Bio-Rad). The primer sequences and numbers of universal probes used in this study were as follows: *Il6* (left: 5'-atcctctggaaccccacac-3', right: 5'-gaactttcgtactgatcctcgtg-3', universal probe: # 53), *Ifna* (left: 5'-tcaagccatccttgtgctaa-3', right: 5'-gtcttttgatgtgaagaggttcaa-3', universal probe: # 3); *Ifnb* (left: 5'-ctggcttccatcatgaacaa-3', right: 5'-agagggctgtggtggagaa-3', universal probe: # 18); *Il12a* (p35) (left: 5'-tcagaatcacaaccatcagca-3', right: 5'-cgccattatgattcagagactg-3', universal probe: # 49); *Il12b* (p40) (left: 5'-tgaactggcgttggaagc-3', right: 5'-gcgggtctggtttgatga-3', universal probe: # 74); *Arg1* (left: 5'-cctgaaggaactgaaaggaaag-3', right: 5'-ttggcagatatgcagggagt-3', universal probe: # 2); *Il10* (left: 5'-cagagccacatgctcctaga-3', right: 5'-tgtccagctggtcctttgtt-3', universal probe: # 41); and *Actb* (left: 5'-aaggccaaccgtgaaaagat-3', right: 5'-gtggtacgaccagaggcatac-3', universal probe: # 56). Sample signals were normalized to the reference gene *Actb* using the

$^{\Delta\Delta}$Ct method: $^{\Delta}Ct = {}^{\Delta}Ct_{sample} - {}^{\Delta}Ct_{reference}$. Percentages relative to the control sample were then calculated for each sample.

Flow cytometry

The surface expression levels of CD11c, CD11b, CD8a, CD44, CD62L, I-Ad, H-2Kd, and CD274 were evaluated by FACSCanto II (BD Biosciences) and the results were analyzed with FlowJo software (Tree Star, Ashland, OR, USA). The mean fluorescence intensity (MFI) ratio (sample ΔMFI (specific marker MFI − isotype control MFI)/control sample ΔMFI × 100) was calculated for samples. A FACSAriaII (BD Biosciences) was used for the isolation of $CD11c^+$ cells from areas of metastatic tissue in the livers of *Il6*$^{+/+}$ or *Il6*$^{-/-}$ mice.

Cytotoxicity assay

Freshly isolated lymphocytes from metastatic livers were incubated with CT26-GFP cells as target cells for 4 h. The percentage cytotoxicity of the collected cells as antitumor effector cells was calculated by counting GFP^+7AAD^+ cells by flow cytometry.

Intracellular cytokine staining

To detect cytoplasmic perforin and granzyme B expression levels in $CD8^+$ T cells,

single cell suspensions from liver tissue (1×10^6 cells/well in a 12-well culture plate) were stimulated with PMA (25 ng/mL) and A23187 calcium ionophore (1 μg/mL) for 4 h in the presence of brefeldin A. Then, the cells were harvested and stained with anti-CD8 mAb and 7-AAD, and fixed with 4% paraformaldehyde. After permeabilization, the fixed cells were stained with anti-Granzyme B or perforin mAbs. To detect cytoplasmic pSTAT1 in CT26 cells, single cell suspensions from liver tissue (1×10^6 cells/well in a 12-well culture plate) were harvested and stained with anti-CD45 mAb and 7-AAD, and fixed with 4% paraformaldehyde. After permeabilization, the fixed cells were stained with pSTAT1 mAb. Data were acquired by flow cytometry.

Immunohistochemistry (IHC)

Metastatic livers obtained from CT26-inoculated *Il6*$^{+/+}$ and *Il6*$^{-/-}$ mice at day 14 were fixed in 4% paraformaldehyde phosphate buffer solution and then embedded in paraffin. After deparaffinization, antigen retrieval for CD3 and CD11c was performed with a reagent kit (pH 9.0) (415211, Nichirei Bioscience, Inc., Tokyo, Japan) at 95°C for 10 min or with proteinase K solution (S3004, Dako, Hamburg, Germany) at room temperature for 5 min, respectively. Endogenous peroxidase activity was blocked by incubating samples with 3% hydrogen peroxide at room temperature for 10 min. After washing with Tris-buffered saline, sections were incubated with anti-CD3 (ab134096;

Abcam) or anti-CD11c (GTX74940; GeneTex) antibodies overnight at 4°C. Sections for CD3 and CD11c staining were incubated at room temperature for 30 min with Histofine Simple Stain MAX PO (R) (424144, Nichirei Bioscience, Inc., Tokyo, Japan) at room temperature for 30 min or with rabbit anti-hamster IgG (6215-01, Southern Biotechnology Associates, Inc.) at room temperature for 30 min, Histofine Simple Stain MAX PO (R) (424144, Nichirei Bioscience, Inc.) at room temperature for 30 min, TSA PLUS Biotin Kit (NEL749A001, Perkin Elmer, Inc., MA) at room temperature for 5 min, and Vectastain Elite ABC Reagent (PK6100, Vector Laboratories, Inc., CA) at room temperature for 30 min. Protein expression was visualized using 3-3'-diaminobezidine-4HCL at room temperature for 5 min. Antigen retrieval for phospho-STAT1 was performed with a reagent kit (pH 9.0) (415211, Nichirei Bioscience, Inc.) at 95°C for 20 min. Endogenous peroxidase activity was blocked by incubation with 0.3% hydrogen peroxide at room temperature for 10 min. After washing with rebuffed saline, sections were treated with anti-phospho-STAT1 (#9167, Cell Signaling Technology, Danvers, Massachusetts, USA) antibody overnight at 4°C. Protein expression was visualized using N-Histofine Simple Stain MAX PO (R) (Nichirei Biosciences, Inc., Tokyo, Japan). After washing, protein expression was visualized using 3-3'-diaminobezidine-4 HCL at

room temperature for 5 min. Finally, all sections were counterstained with Mayer's hematoxylin.

Tumor specimens from 108 CRC patients were formalin-fixed and paraffin-embedded and sections were stained with hematoxylin-eosin (HE). The slides were treated with anti-IL-6 (ab6672, at 1:500 dilution, Abcam) and anti-PD-L1 (SP142, at 1:150 dilution, Spring, Bioscience, Inc.) antibodies. Protein expression was visualized using N-Histofine Simple Stain MAX PO (R) (Nichirei Biosciences, Inc., Tokyo, Japan) and peroxidase (Envision/HRP; Dako, Tokyo, Japan), respectively. After washing, IL-6 and PD-L1 protein expression was visualized using 3-3'-diaminobezidine-4 HCL at room temperature for 5 min and 10 min, respectively. Finally, all sections were counterstained with Mayer's hematoxylin.

IL-6 and PD-L1 immunohistochemical evaluation

All assessments were made on viable tumor specimens at ×400 magnification. Each slide was evaluated by a pathologist who was blinded to the clinical outcomes.

Statistical analysis

In vitro experiments were repeated 3–5 times. *In vivo* experiments consisting of 4–10 mice per group were independently performed 2–3 times. For survival studies, we used

10–30 mice per experimental group. Single representative experiments are indicated in the figures. Mean values and SDs were calculated for each dataset. Significant differences in the results were determined by a one-way analysis of variance (ANOVA) and Dunnett's post-test. In some experiments, the two-tailed Student's t-test was used to evaluate differences between two groups. P-values < 0.05 were considered statistically significant using the two-sided Student's t-test. The log-rank test was used to determine statistically significant differences in survival curves among CT26-inoculated mice and CRC patients. The prognostic implications of IL-6 and PD-L1 expression and clinicopathological parameters were analyzed by Cox univariate and multivariate proportional hazard models. Data were analyzed using JMP statistical software for Windows (version 13.1.0; SAS Institute Inc., Cary, NC, USA).

Results

IL-6 produced in tumor-bearing hosts augments metastatic colonization of colon cancer cells

To investigate the effect of IL-6 on the metastatic colonization of colon cancer cells in liver tissue, we intrasplenically inoculated GFP-transduced CT26 murine colon cancer cells into wild-type BALB/c (*Il6*$^{+/+}$) and BALB/c background IL-6-deficient (*Il6*$^{-/-}$) mice (Fig. 1A). Serum IL-6 levels were increased in *Il6*$^{+/+}$ but not *Il6*$^{-/-}$ mice at 14 days after inoculation (Fig. 1B). In addition, serum alanine transaminase (ALT) and aspartate transaminase (AST) levels were higher in *Il6*$^{+/+}$ mice than in *Il6*$^{-/-}$ mice (Fig. 1C). The percentages of liver weight per total body weight of tumor-bearing *Il6*$^{+/+}$ mice were significantly heavier than that of *Il6*$^{-/-}$ mice (Fig. 1D). HE staining revealed that the metastatic foci of CT26 in *Il6*$^{+/+}$ mice were thicker than in *Il6*$^{-/-}$ mice (Fig. 1E and F). *In vivo* imaging analysis of liver tissue showed that the tumorigenesis of CT26 cells was significantly reduced in *Il6*$^{-/-}$ mice compared with *Il6*$^{+/+}$ mice (Fig. 1G and H). Furthermore, the survival of *Il6*$^{+/+}$ mice was significantly shorter compared with *Il6*$^{-/-}$ mice (Fig. 1I). Next, we performed intravenous injection of CT26 cells into *Il6*$^{+/+}$ mice and *Il6*$^{+/+}$ mice to evaluate the effect of IL-6 on the metastatic colonization of colon cancer cells in the lung. Metastatic colonization in the lungs of *Il6*$^{-/-}$ mice was significantly reduced compared with *Il6*$^{+/+}$ mice (Fig. S1A–D). Moreover, the survival of

CT26-bearing *Il6*$^{-/-}$ mice was significantly prolonged compared with that of *Il6*$^{+/+}$ mice (Fig. S1E). These data suggest that IL-6 promotes the metastatic colonization of colon cancer cells in the lung as well as in liver tissue. Furthermore, we intrasplenically inoculated GFP-transduced 4T1 breast cancer cells into *Il6*$^{+/+}$ and *Il6*$^{-/-}$ mice to investigate the effect of IL-6 on the metastatic colonization of breast cancer cells in the livers. Metastatic colonization of 4T1 cells in the livers of *Il6*$^{-/-}$ mice was significantly reduced compared with *Il6*$^{+/+}$ mice (Fig. S2A–D). The survival of 4T1 intrasplenically-injected *Il6*$^{-/-}$ mice was significantly prolonged compared with that of *Il6*$^{+/+}$ mice (Fig. S2E). These data suggest that IL-6 promotes the metastatic colonization of breast cancer cells as well as colon cancer cells in the liver *in vivo*.

To confirm the effect of cancer cell-produced IL-6 on metastatic colonization, we injected anti-IL-6 mAb into our *Il6*$^{+/+}$ mouse model. As a result, we confirmed that the administration of anti-IL-6 mAb significantly suppressed the metastatic colonization of CT26 colon cancer cells in the liver (Fig. S3A–D) and prolonged the survival of CT26-bearing *Il6*$^{+/+}$ mice (Fig. S3E). Based on these data, we speculated that both host mouse- and CT26 cancer cell-derived IL-6 might be involved in the metastatic colonization of the liver tissue of our experimental model. In addition, we investigated *Il6* gene expression levels in whole cells and CT26 cells isolated from the liver tissues of tumor-bearing *Il6*$^{-/-}$ and *Il6*$^{+/+}$ mice. *Il6* expression in whole cells was higher

compared with that in CT26 cells isolated from the liver tissue of *Il6*$^{+/+}$ mice, although *Il6* levels in whole cells from *Il6*$^{-/-}$ mice were not significantly different to that of CT26 cells isolated from *Il6*$^{-/-}$ mice (Fig. S4). *Il6* expression levels in CT26 cells isolated from *Il6*$^{+/+}$ mice were higher compared with CT26 cells from the liver tissue of *Il6*$^{-/-}$ mice. These data suggest that IL-6 derived from mice may augment *Il6* expression levels in CT26 colon cancer cells *in vivo*.

In this study, we established *Il6* gene-knockout CT26 (CT26-*Il6*KO) cells (Fig. S5A), which had a lower proliferative ability *in vitro* compared with control CT26-mock cells (Fig. S5B). When these cells were intrasplenically inoculated into *Il6*$^{+/+}$ BALB/c mice, the metastatic colonization of CT26-*Il6*KO cells in the liver was significantly reduced compared with the control cells (Fig. S5C and D). Next, CT26-*Il6*KO cells were injected into *Il6*$^{+/+}$ and *Il6*$^{-/-}$ mice. We confirmed that the metastatic colonization of CT26-*Il6*KO cells in the livers of *Il6*$^{-/-}$ mice was significantly reduced compared with those of *Il6*$^{+/+}$ mice (Fig. 1J and K). These findings suggest that IL-6 produced from the tumor-bearing host as well as CT26 cancer cells facilitates the metastatic colonization of colon cancer cells *in vivo*.

Maturation of CD11c^{+} DCs and killer functions of CD8^{+} T cells are enhanced in the liver metastases of *Il6*$^{-/-}$ mice

Next, we examined the immune status of mice with CT26 colon cancer cell metastatic colonization. $CD11c^+$ and $CD3^+$ cells were accumulated in the tumorous regions of liver tissue (Fig. 2A). Furthermore, I-$Ad^{high}CD11c^+$ mature DCs and $CD44^{high}CD62L^-$ effector memory $CD8^+$ T cells had infiltrated into the CT26-bearing liver tissue of *Il6*$^{-/-}$ mice to a greater degree than that in *Il6*$^{+/+}$ mice (Fig. 2B). *Il12a*, *Ib12b*, *Ifna*, and *Ifnb* expression in $CD11c^+$ cells isolated from the liver metastases of *Il6*$^{-/-}$ mice were higher than those of *Il6*$^{+/+}$ mice, whereas *Arg1* and *Il10* expression in *Il6*$^{+/+}$ mice was higher than that in *Il6*$^{-/-}$ mice (Fig. 2C). The cytotoxicity of immune cells collected from the liver tissue of *Il6*$^{-/-}$ mice was higher than that of *Il6*$^{+/+}$ mice (Fig. 2D). Next, we confirmed that both perforin and granzyme B levels in $CD8^+$ T cells that had infiltrated into the liver metastases of *Il6*$^{-/-}$ mice were significantly higher than those of *Il6*$^{+/+}$ mice (Fig. 2E). These data suggested that the functions of anti-tumor effector cells including mature $CD11c^+$ DCs and $CD8^+$ killer T cells were augmented in the CT26-bearing liver tissue of *Il6*$^{-/-}$ mice.

IL-12-mediated activation of $CD8^+$ killer T cells is involved in the reduction of metastatic colonization of CT26 colon cancer cells in the liver tissue of *Il6*$^{-/-}$ mice

We then investigated the anti-tumor effector cells in this model. *In vivo* injection of clodronate liposomes into *Il6*$^{-/-}$ mice to deplete phagocytes including DCs and

macrophages significantly enhanced the metastatic colonization of CT26 colon cancer cells in the liver (Fig. 3A–C). The depletion enhanced the metastatic colonization in the livers of *Il6*$^{+/+}$ mice (Fig. S6A-C), however the difference was much more pronounced in the *Il6*$^{-/-}$ setting. In addition, the depletion of CD8^{+} T cells by the administration of anti-CD8 mAb significantly increased the metastatic colonization of CT26 cells in the livers of *Il6*$^{-/-}$ mice (Fig. 3D–F), whereas the depletion did not significantly increase in the livers of *Il6*$^{+/+}$ mice (Fig. S6D–F). To address the contribution of CD4^{+} T cells to this effect, anti-CD4 mAb was administered to the *Il6*$^{-/-}$ liver metastasis model. The depletion of CD4^{+} T cells reduced the liver metastasis of CT26 cells in *Il6*$^{-/-}$ mice (Fig. S7A–C). We then injected anti-CD4 mAb into *Il6*$^{+/+}$ mice and found that the depletion of CD4^{+} T cells significantly reduced the metastatic colonization of CT26 cells in the liver (Fig. S7D–F). Furthermore, we confirmed that the *in vivo* injection of anti-CD4 mAb into *Il6*$^{+/+}$ mice significantly enhanced the infiltration of I-Ad^{high}CD11c^{+} mature DCs, CD44^{high}CD62L^{-} effector memory CD8^{+} T cells, and perforin-positive CD8^{+} T cells into liver metastases (Fig. S7G and H). These results suggest that CD8^{+} T cells are required for the suppression of metastatic colonization of the livers of *Il6*$^{-/-}$ mice.

In addition, we found that IL-6-deficient conditions augmented both *Il12a* and *Il12b* expression levels in CD11c^{+} cells in metastatic regions within liver tissue (Fig. 2C). Previous reports indicated that IL-12 production by mature DCs induced anti-

tumor effector cells through cell–cell interactions in tumor-bearing hosts (17, 18). To investigate the effect of IL-12 production on metastatic colonization in the livers of *Il6*$^{-/-}$ mice, we administered anti-IL-12 mAb to *Il6*$^{-/-}$ mice and observed significantly enhanced metastatic colonization of intrasplenically injected CT26 cells in the liver (Fig. 3G–I), whereas the depletion did not enhance in the livers of *Il6*$^{+/+}$ mice (Fig. S6D-F). We also noted the accumulation of CD11c^{+} and CD3^{+} cells in liver metastases (Fig. 3J) and confirmed that the infiltration of I-Ad^{high}CD11c^{+} mature DCs and CD44^{high}CD62L^{-} effector memory CD8^{+} T cells was significantly reduced by the administration of anti-IL-12 mAb to *Il6*$^{-/-}$ mice (Fig. 3K). The administration of anti-IL-12 mAb significantly reduced the cytotoxicity of immune cells, as well as the levels of perforin and granzyme B in CD8^{+} T cells in liver metastases compared with *Il6*$^{-/-}$ mice injected with control antibody (Fig. 3L and M). These results indicated that augmented IL-12 production in the liver tissue of *Il6*$^{-/-}$ mice was related to the enhanced anti-tumor effector function of CD8^{+} T cells to prevent metastatic colonization in tumor-bearing hosts.

Metastatic colonization is reduced by augmenting type I IFN signaling through IFN-AR1, which upregulates MHC class I and PD-L1 in colon cancer cells in *Il6*$^{-/-}$ mice

Ifna and *Ifnb* expression levels in CD11c^{+} DCs were enhanced in the tumor-bearing

livers of *Il6*$^{-/-}$ mice (Fig. 2C). To confirm the involvement of type I IFN production in the reduction of metastatic colonization, we injected anti-IFN-AR1 antagonistic mAb into the liver metastatic colonization *Il6*$^{-/-}$ mouse model. The blockade of type I IFN signaling through IFN-AR1 elevated the metastatic colonization of CT26 colon cancer cells in the livers of *Il6*$^{-/-}$ mice (Fig.4A-C). We confirmed that the surface level of H-2K^{d}, an MHC class I molecule, on CT26 colon cancer cells was significantly increased after stimulation with IFN-α and IFN-β in a STAT-1 dependent manner *in vitro* (Fig. 4D). Previous studies reported that stimulation with IFN-γ upregulated surface PD-L1 and MHC class I levels on cancer cells (19-21). In this study, we found that stimulation with IFN-α and IFN-β augmented the surface level of PD-L1 on CT26 colon cancer cells (Fig. 4E). The upregulation of PD-L1 expression was partially blocked by a STAT1 inhibitor, and immunohistochemical analysis revealed that STAT1 was activated in the tumor sites of *Il6*$^{-/-}$ mice (Fig. 4F). Flow cytometry data showed that the levels of phospho-STAT1 in CT26 cells in the liver metastases of *Il6*$^{-/-}$ mice were significantly higher than in *Il6*$^{+/+}$ mice (Fig. 4G). Furthermore, we confirmed that surface PD-L1 and MHC class I levels on CT26 cells in the liver metastases of *Il6*$^{-/-}$ mice were significantly higher compared with *Il6*$^{+/+}$ mice (Fig. 4H). These findings suggested that type I IFN signaling was upregulated in the liver tissue of *Il6*$^{-/-}$ mice to activate antitumor immunity, which also resulted in the induction of PD-L1 as well as MHC class I expression on

colon cancer cells in tumor-bearing states.

In vivo injection of anti-PD-L1 mAb augments anti-tumor immunity in the livers of *Il6*$^{-/-}$ mice

To examine the effect of PD-L1 induction on liver metastatic CT26 cells in *Il6*$^{-/-}$ mice, we injected anti-PD-L1 mAb into our mouse model. The administration of anti-PD-L1 mAb significantly reduced the metastatic colonization of CT26 cells in the liver tissue of *Il6*$^{-/-}$ mice at 19 days after inoculation (Fig. 5A–C). Furthermore, we observed the accumulation of CD11c^{+} and CD3^{+} cells in metastatic regions in liver tissue (Fig. 5D) and confirmed that the infiltration of I-Ad^{high}CD11c^{+} mature DCs and CD44^{high}CD62L^{-} effector memory CD8^{+} T cells was significantly increased by the administration of anti-PD-L1 mAb into *Il6*$^{-/-}$ mice (Fig. 5E). Treatment with anti-PD-L1 mAb enhanced the cytotoxicity of immune cells as well as the levels of perforin and granzyme B in CD8^{+} T cells that had infiltrated the liver metastases when compared with control antibody (Fig. 5F and G). Furthermore, the survival of CT26-bearing *Il6*$^{-/-}$ mice was significantly prolonged by the administration of anti-PD-L1 mAb compared with control IgG-treated mice (Fig. 5H). We then examined the effect of anti-PD-L1 mAb on our metastatic colonization model using *Il6*$^{+/+}$ mice. We found that PD-L1 blockade did not reduce the metastatic colonization of CT26 cells in the livers of *Il6*$^{+/+}$ mice (Fig. S8A–F). These

findings suggested that a lack of IL-6 under tumor-bearing conditions augmented anti-tumor immunity involving PD-L1 induction in cancer cells, and facilitated immune checkpoint inhibition therapy using anti-PD-L1 mAb to prevent the liver metastasis of colon cancer cells.

IL-6 expression in the primary tumor sites of CRC patients correlates with disease-free survival in both PD-L1-positive and -negative cases

Finally, we conducted an immunohistochemical study on the IL-6 and PD-L1 levels in the tumor tissues of CRC patients (Supplementary Table S1). As described in the Materials and Methods, 108 cases of CRC were stratified according to negative and positive expression of IL-6 and PD-L1 (Fig. 6A). Statistical analysis revealed that disease-free survival (DFS) was significantly prolonged in IL-6-negative patients (n = 55) compared with IL-6-positive patients (n = 53) (P = 0.006) (Fig. 6B and Supplementary Table S2). However, PD-L1-positive patients (n = 71) had relatively unfavorable DFS (P = 0.051) compared with PD-L1-negative patients (n = 37) (Fig. 6B and Supplementary Table S2). We confirmed that IL-6 positivity in both PD-L1-negative patients (n = 39) and PD-L1-positive patients (n = 14) was associated with significantly unfavorable DFS compared with IL-6 negativity in both PD-L1-negative patients (n = 32, P = 0.041) and PD-L1-positive patients (n = 23, P = 0.009) (Fig. 6C). To evaluate

IL-6 expression as an independent prognostic factor, we performed a univariate analysis of the 108 CRC patients using the Cox proportional hazards model. We found that pathological T stage, N stage, lymphatic and venous invasion, CEA, CA19-9, and IL-6 were significantly correlated with recurrence. Multivariate analysis confirmed IL-6 was a significant predictor of DFS (relative risk 1.958, 95% CI, 1.004–3.999, $P = 0.049$) (Supplementary Table S2). Furthermore, we conducted an immunohistochemical study of IL-6 and PD-L1 levels in the liver metastases of CRC patients. Fifty-seven liver metastases samples from CRC patients were stratified by the negative and positive expression of IL-6 and PD-L1 (Fig. S9A). Statistical analysis revealed that DFS did not significantly differ between IL-6-negative (n = 22) and IL-6-positive (n = 35) patients ($P = 0.929$) (Fig. S9B). Moreover, DFS was not significantly prolonged in PD-L1-negative patients (n = 31) compared with PD-L1-positive patients (n = 26) ($P = 0.446$) (Fig. S9B). These data suggest that IL-6 expression in the primary tumor sites of CRC is associated with the recurrence of CRC cells including liver metastasis.

Discussion

CRC, a common cancer worldwide, has a high recurrence rate after surgery that remains to be resolved (13, 14). Because liver metastasis is a major cause of CRC-associated deaths (22), elucidation of the precise mechanism involved in liver metastasis is required for more effective treatment of patients with CRC. Our results indicate that IL-6 modulates the immune status of the tumor microenvironment, which facilitates metastatic colonization of colon cancer cells in the liver by causing the dysfunction of anti-tumor effector cells.

It was reported that chronic inflammation is closely related to tumorigenesis and cancer progression (23-25). Previous studies revealed that high levels of serum IL-6, a major proinflammatory cytokine, are associated with poor prognosis in metastatic colon cancer patients (26) and refractoriness to treatments for carcinomas (27, 28). Furthermore, IL-6 augmented growth and epithelial-mesenchymal transition, metastatic spread (29-30), tumor angiogenesis, and the renewal and drug resistance of some cancer stem cells (31-33). In the current study, we revealed that IL-6 produced in a tumor-bearing host promoted the metastatic colonization of colon cancer cells by suppressing anti-tumor immunity. From these findings, we speculate that IL-6 has a critical role in anti-tumor immunity by controlling the metastasis of cancer cells *in vivo*.

In our metastatic colonization model, we found that depletion of $CD4^+$T cells

enhanced anti-tumor effect in *Il6*$^{+/+}$ mice, however the efficacy was limited in *Il6*$^{-/-}$ mice. A previous paper revealed that CD4^{+} T cells in lymph nodes and tumor-infiltrating CD4^{+}T and CD8^{+}T cells preferentially produced IFN-γ in CT26 intradermally-injected *Il6*$^{-/-}$ mice compared with *Il6*$^{+/+}$ mice (21). It is well-known that IFN-γ suppresses the differentiation and function of Treg cells. Together with the data in this study, we speculated that immunosuppressive Treg cells may not function in *Il6*$^{-/-}$ mice, whereas Treg cells were generated in *Il6*$^{+/+}$ mice in our metastatic colonization model.

We found that *Il12* expression in CD11c^{+} DCs as well as the killer function of CD8^{+} T cells were augmented under IL-6-deficient mice in our liver metastatic colonization model (Fig. 2C). IL-12 is a critical cytokine that mediates anti-tumor effects by activating both NK cells (34) and cytotoxic CD8^{+} T lymphocytes (35). Tumor gene therapy with *Il12* was effective for colorectal liver metastasis treatment in an experimental mouse model (36). In our model using IL-6-deficient mice, the neutralization of IL-12 significantly enhanced the metastatic colonization of colon cancer cells and suppressed the killer function of tumor-infiltrating CD8^{+} T cells in the liver (Fig. 3G–M). Previous studies demonstrated that IL-6 suppressed the maturation of DCs, resulting in a reduction in antigen presentation that is normally required for the induction of antigen-specific T cells (8, 12). Therefore, we speculate that IL-6 production in tumor-bearing hosts suppresses IL-12 production by DCs, which is

essential for the activation of anti-tumor effector T cells, and that this promotes the subsequent metastatic colonization of colon cancer cells in the liver.

In this study, we found that *Ifna* and *Ifnb* expression in $CD11c^+$ cells and the surface level of MHC class I of colon cancer cells were enhanced in the liver tissues of our metastatic colonization model using *Il6*$^{-/-}$ mice (Fig. 2C and 4H). A previous study using mouse models indicated that CRC colonization in the liver was suppressed by *Ifna* gene and cell therapies (37). In our study, blockade of IFN-AR1-mediated type I IFN signaling led to an increase in metastatic colonization in the livers of *Il6*$^{-/-}$ mice (Fig. 4A–C). Therefore, we hypothesize that IL-6 produced in tumor-bearing hosts suppresses the production of type I IFNs by host cells including DCs and reduces the levels of MHC class I expression on cancer cells. This in turn promotes the metastatic colonization of colon cancer cells by reducing the recognition of target cancer cells by anti-tumor effector T cells.

Previous studies reported that stimulation with IFN-γ upregulated surface PD-L1 and MHC class I levels on cancer cells (19-21). In our experiments, *in vitro* stimulation with IFN-α and IFN-β increased the surface levels of PD-L1 as well as MHC class I on CT26 colon cancer cells (Fig. 4D and E). Furthermore, we confirmed that a lack of IL-6 in tumor-bearing hosts enhanced IFN-AR1-mediated type-I IFN signaling and augmented PD-L1 levels on CT26 colon cancer cells (Fig. 4F–H), whereas metastatic

colonization was significantly reduced compared with IL-6-sufficent conditions (Fig. 1E–H, J, and K). Our previous study indicated that anti-tumor effector cells including $CD8^+$ T cells accumulated at higher levels in the tumor tissue of IL-6-deficient mice (21). From these data, we speculated that administration of anti-PD-L1 mAb might be more effective at inhibiting the metastatic colonization of colon cancer cells in the livers of *Il6*$^{-/-}$ mice that caused the upregulation of PD-L1 expression in an IFN-α/β-IFN-AR1-dependent manner. As expected, metastatic colonization was significantly inhibited by treatment of *Il6*$^{-/-}$ mice (Fig. 5) with anti-PD-L1 mAb, but not *Il6*$^{+/+}$ mice (Fig. S8), whereby a lack of IL-6 led to the activation of anti-tumor effector T cells that prolonged the survival rate of the mice.

When choosing the optimum therapy for cancer patients, it is important to evaluate their immune status (38). In our study using clinical specimens from CRC patients, low IL-6 levels in primary tumor tissues (PD-L1-negative and -positive tumors) were significantly associated with good DFS, suggesting that such cases had a beneficial anti-tumor immune status (Fig. 6 and Supplementary Table S2). A recent study reported that high PD-L1 levels on tumor cells negatively affected the survival of CRC patients (39). Other reports indicated that high levels of PD-L1 in colorectal carcinoma (40-42) and other cancer types (43-45) were associated with significantly improved survival. Therefore, the relationship between PD-L1 level and the survival of

CRC patients remains controversial (46). Based on previous reports and our findings in the present study, we speculated that IL-6 levels in primary tissues might be a good marker to evaluate the immune status of both PD-L1-negative and -positive CRC patients, which may provide useful information for determining the type of cancer therapy required, such as immune checkpoint inhibitors targeting PD-1/PD-L1, and for the prognosis of recurrent tumors including liver metastasis.

In terms of therapeutic effects, a previous report demonstrated that the targeted inhibition of IL-6 enhanced the efficacy of anti-PD-L1 antibody in murine models of pancreatic cancer (47). A recent clinical study using an anti-IL-6R mAb, tocilizumab, with carboplatin/doxorubicin and IFN-α2b was conducted in patients with recurrent epithelial ovarian cancer (48). They reported that myeloid cells in IL-6R mAb-treated patients produced more IL-12 and that T cells were highly activated and secreted large amounts of effector cytokines, indicating a beneficial change in the anti-tumor immune status of the human subjects. The results of our metastatic colonization model with IL-6-deficient mice are consistent with these findings. However, a limitation to our metastasis model is that it does not fully reflect multistep process of metastasis because this is an experimental colonization assay which could skip the process in which cancer cells detached from the primary site intravasate into vessels.

In conclusion, IL-6 from tumor-bearing hosts suppresses the effective induction

of anti-tumor immunity and promotes the colonization of metastasis in cancerous liver lesions. Lack of IL-6 augments the effector functions of DCs and killer T cells that infiltrate tumor microenvironments. From these results, we speculate that the IL-6 signaling cascade might be a new target to regulate the liver metastasis of colon cancer cells in CRC patients through the augmentation of anti-tumor effector cells.

Disclosure of Potential Conflicts of Interest

No potential conflicts of interest were disclosed.

Authors' Contributions

Conception and design: H. Kitamura, A. Taketomi

Development of methodology: Y. Toyoshima, H. Kitamura, A. Taketomi

Acquisition of data (animal provision, acquisition and management of patients, facilities provision, etc.): Y. Toyoshima, H. Kitamura, A. Taketomi, Y. Ohno, S. Honma, H. Kawamura, N. Takahashi, T. Kamiyama

Analysis and interpretation of data (e.g., statistical analysis, biostatistics, computational analysis): Y. Toyoshima, H. Kitamura, H. Xiang, Y. Ohno, S. Honma, T. Kamiyama, M. Tanino, A. Taketomi

Writing, review, and/or revision of the manuscript: Y. Toyoshima, H. Kitamura, A. Taketomi

Administrative, technical, or material support (i.e., reporting or organizing data, constructing databases): Y. Toyoshima, H. Kitamura, A. Taketomi

Study supervision: H. Kitamura, A. Taketomi

Acknowledgments

We thank Dr. K. Sugiyama, S. Kii, Dr. N. Okada, Dr. N. Ichikawa, and Dr. T. Yoshida for their excellent technical assistance and and thoughtful advice on this study. This work was partially supported by Grants-in-Aid for Scientific Research (C) (25460584 to H. Kitamura and 16K10526 to N. Takahashi) from the Japan Society for the Promotion of Science (JSPS), the Platform Project for Supporting Drug Discovery and Life Science Research (Platform for Drug Discovery, Informatics, and Structural Life Science) from the Ministry of Education, Culture, Sports, Science and Technology (MEXT) of Japan (to H. Kitamura), the Japan Agency for Medical Research and Development (AMED) (to A. Taketomi), and the Joint Research Program of the Institute for Genetic Medicine, Hokkaido University (to M. Tanino and A. Taketomi). We thank H. Nikki March, PhD, from Edanz Group (www.edanzediting.com/ac) for editing a draft of this manuscript.

References

1. Larkin J, Chiarion-Sileni V, Gonzalez R, Grob JJ, Cowey CL, Lao CD*, et al.* Combined Nivolumab and Ipilimumab or Monotherapy in Untreated Melanoma. *N Engl J Med* **2015**;373:23-34.

2. Topalian SL, Drake CG, Pardoll DM. Immune checkpoint blockade: a common denominator approach to cancer therapy. Cancer cell **2015**;27:450-61.

3. Binnewies M, Roberts EW, Kersten K, Chan V, Fearon DF, Merad M*, et al.* Understanding the tumor immune microenvironment (TIME) for effective therapy. *Nat Med* **2018**;24:541-50.

4. Spranger S, Gajewski TF. Impact of oncogenic pathways on evasion of antitumour immune responses. *Nat Rev Cancer* **2018**;18:139-47.

5. Hirano T, Yasukawa K, Harada H, Taga T, Watanabe Y, Matsuda T*, et al.* Complementary DNA for a novel human interleukin (BSF-2) that induces B lymphocytes to produce immunoglobulin. *Nature* **1986**;324:73-6.

6. Tanaka T, Kishimoto T. The biology and medical implications of interleukin-6. *Cancer Immunol Res* **2014**;2:288-94.

7. Yu H, Pardoll D, Jove R. STATs in cancer inflammation and immunity: a leading role for STAT3. *Nat Rev Cancer* **2009**;9:798-809.

8. Park SJ, Nakagawa T, Kitamura H, Atsumi T, Kamon H, Sawa S*, et al.* IL-6 regulates

in vivo dendritic cell differentiation through STAT3 activation. *J Immunol* **2004**;173:3844-54.

9. Kitamura H, Kamon H, Sawa S, Park SJ, Katunuma N, Ishihara K*, et al.* IL-6-STAT3 controls intracellular MHC class II alphabeta dimer level through cathepsin S activity in dendritic cells. *Immunity* **2005**;23:491-502.
10. Sumida K, Wakita D, Narita Y, Masuko K, Terada S, Watanabe K*, et al.* Anti-IL-6 receptor mAb eliminates myeloid-derived suppressor cells and inhibits tumor growth by enhancing T-cell responses. *Eur J I* **2012**;42:2060-72.
11. Narita Y, Kitamura H, Wakita D, Sumida K, Masuko K, Terada S*, et al.* The key role of IL-6-arginase cascade for inducing dendritic cell-dependent CD4(+) T cell dysfunction in tumor-bearing mice. *J Immunol* **2013**;190:812-20.
12. Ohno Y, Kitamura H, Takahashi N, Ohtake J, Kaneumi S, Sumida K*, et al.* IL-6 down-regulates HLA class II expression and IL-12 production of human dendritic cells to impair activation of antigen-specific CD4(+) T cells. *Cancer Immunol Immunother* **2016**;65:193-204.
13. Ferlay J, Soerjomataram I, Dikshit R, Eser S, Mathers C, Rebelo M*, et al.* Cancer incidence and mortality worldwide: sources, methods and major patterns in GLOBOCAN 2012. *Int J Cancer* **2015**;136:E359-86.
14. Arnold M, Sierra MS, Laversanne M, Soerjomataram I, Jemal A, Bray F. Global

patterns and trends in colorectal cancer incidence and mortality. *Gut* **2017**;66:683-91.

15. Lambert AW, Pattabiraman DR, Weinberg RA. Emerging Biological Principles of Metastasis. *Cell* **2017**;168:670-91.
16. Kitamura T, Qian BZ, Pollard JW. Immune cell promotion of metastasis. *Nat Rev Immunol* **2015**;15:73-86.
17. Kitamura H, Iwakabe K, Yahata T, Nishimura S, Ohta A, Ohmi Y*, et al.* The natural killer T (NKT) cell ligand alpha-galactosylceramide demonstrates its immunopotentiating effect by inducing interleukin (IL)-12 production by dendritic cells and IL-12 receptor expression on NKT cells. *J Exp Med* **1999**;189:1121-8.
18. Fujii S, Shimizu K, Smith C, Bonifaz L, Steinman RM. Activation of natural killer T cells by alpha-galactosylceramide rapidly induces the full maturation of dendritic cells in vivo and thereby acts as an adjuvant for combined CD4 and CD8 T cell immunity to a coadministered protein. *J Exp Med* **2003**;198(2):267-79.
19. Mandai M, Hamanishi J, Abiko K, Matsumura N, Baba T, Konishi I. Dual Faces of IFNgamma in Cancer Progression: A Role of PD-L1 Induction in the Determination of Pro- and Antitumor Immunity. *Clin Cancer Res* **2016**;22:2329-34.
20. Abiko K, Matsumura N, Hamanishi J, Horikawa N, Murakami R, Yamaguchi K*, et al.* IFN-gamma from lymphocytes induces PD-L1 expression and promotes

progression of ovarian cancer. *Br J Cancer* **2015**;112:1501-9.

21. Ohno Y, Toyoshima Y, Yurino H, Monma N, Xiang H, Sumida K*, et al.* Lack of interleukin-6 in the tumor microenvironment augments type-1 immunity and increases the efficacy of cancer immunotherapy. *Cancer Sci* **2017**;108:1959-66.
22. Carpizo DR, D'Angelica M. Liver resection for metastatic colorectal cancer in the presence of extrahepatic disease. *Lancet Oncol* **2009**;10: 801-9.
23. Mantovani A, Allavena P, Sica A, Balkwill F. Cancer-related inflammation. *Nature* **2008**;454:436-44.
24. Grivennikov S, Karin E, Terzic J, Mucida D, Yu GY, Vallabhapurapu S*, et al.* IL-6 and Stat3 are required for survival of intestinal epithelial cells and development of colitis-associated cancer. *Cancer cell* **2009**;15:103-13.
25. Crusz SM, Balkwill FR. Inflammation and cancer: advances and new agents. *Nat Rev Clin Oncol* **2015**;12:584-96.
26. Thomsen M, Kersten C, Sorbye H, Skovlund E, Glimelius B, Pfeiffer P*, et al.* Interleukin-6 and C-reactive protein as prognostic biomarkers in metastatic colorectal cancer. *Oncotarget* **2016**;7:75013-22.
27. Mitsunaga S, Ikeda M, Shimizu S, Ohno I, Furuse J, Inagaki M*, et al.* Serum levels of IL-6 and IL-1beta can predict the efficacy of gemcitabine in patients with advanced pancreatic cancer. *Br J Cancer* **2013**;108:2063-9.

28. Makuuchi Y, Honda K, Osaka Y, Kato K, Kojima T, Daiko H*, et al.* Soluble interleukin-6 receptor is a serum biomarker for the response of esophageal carcinoma to neoadjuvant chemoradiotherapy. *Cancer Sci* **2013**;104:1045-51.

29. Lee SO, Yang X, Duan S, Tsai Y, Strojny LR, Keng P*, et al.* IL-6 promotes growth and epithelial-mesenchymal transition of CD133+ cells of non-small cell lung cancer. *Oncotarget* **2016**;7:6626-38.

30. Albino D, Civenni G, Rossi S, Mitra A, Catapano CV, Carbone GM. The ETS factor ESE3/EHF represses IL-6 preventing STAT3 activation and expansion of the prostate cancer stem-like compartment. *Oncotarget* **2016**;7:76756-68.

31. Gopinathan G, Milagre C, Pearce OM, Reynolds LE, Hodivala-Dilke K, Leinster DA*, et al.* Interleukin-6 Stimulates Defective Angiogenesis. *Cancer Res* **2015**;75:3098-107.

32. Nagasaki T, Hara M, Nakanishi H, Takahashi H, Sato M, Takeyama H. Interleukin-6 released by colon cancer-associated fibroblasts is critical for tumour angiogenesis: anti-interleukin-6 receptor antibody suppressed angiogenesis and inhibited tumour-stroma interaction. *Br J Cancer* **2014**;110:469-78.

33. Gilbert LA, Hemann MT. DNA damage-mediated induction of a chemoresistant niche. *Cell* **2010**;143:355-66.

34. Uemura A, Takehara T, Miyagi T, Suzuki T, Tatsumi T, Ohkawa K*, et al.* Natural killer

cell is a major producer of interferon gamma that is critical for the IL-12-induced anti-tumor effect in mice. *Cancer Immunol Immunother* **2010**;59:453-63.

35. Rubinstein MP, Su EW, Suriano S, Cloud CA, Andrijauskaite K, Kesarwani P*, et al.* Interleukin-12 enhances the function and anti-tumor activity in murine and human CD8(+) T cells. *Cancer Immunol Immunother* **2015**;64:539-49.

36. Martinet O, Ermekova V, Qiao JQ, Sauter B, Mandeli J, Chen L*, et al.* Immunomodulatory gene therapy with interleukin 12 and 4-1BB ligand: long- term remission of liver metastases in a mouse model. *J Natl Cancer Inst* **2000**;92:931-6.

37. Catarinella M, Monestiroli A, Escobar G, Fiocchi A, Tran NL, Aiolfi R*, et al.* IFNalpha gene/cell therapy curbs colorectal cancer colonization of the liver by acting on the hepatic microenvironment. *EMBO Mol Med* **2016**;8:155-70.

38. Chen DS, Mellman I. Elements of cancer immunity and the cancer-immune set point. *Nature* **2017**;541:321-30.

39. Koganemaru S, Inoshita N, Miura Y, Miyama Y, Fukui Y, Ozaki Y*, et al.* Prognostic value of programmed death-ligand 1 expression in patients with stage III colorectal cancer. *Cancer Sci* **2017**;108:853-8.

40. Droeser RA, Hirt C, Viehl CT, Frey DM, Nebiker C, Huber X*, et al.* Clinical impact of programmed cell death ligand 1 expression in colorectal cancer. *Eur J Cancer*

2013;49:2233-42.

41. Dunne PD, McArt DG, O'Reilly PG, Coleman HG, Allen WL, Loughrey M*, et al.* Immune-Derived PD-L1 Gene Expression Defines a Subgroup of Stage II/III Colorectal Cancer Patients with Favorable Prognosis Who May Be Harmed by Adjuvant Chemotherapy. *Cancer Immunol Res* **2016**;4:582-91.
42. Li Y, Liang L, Dai W, Cai G, Xu Y, Li X*, et al.* Prognostic impact of programed cell death-1 (PD-1) and PD-ligand 1 (PD-L1) expression in cancer cells and tumor infiltrating lymphocytes in colorectal cancer. *Mol Cancer* **2016**;15:55.
43. Taube JM, Anders RA, Young GD, Xu H, Sharma R, McMiller TL*, et al.* Colocalization of inflammatory response with B7-h1 expression in human melanocytic lesions supports an adaptive resistance mechanism of immune escape. *Sci Transl Med* **2012**;4:127ra37.
44. Darb-Esfahani S, Kunze CA, Kulbe H, Sehouli J, Wienert S, Lindner J*, et al.* Prognostic impact of programmed cell death-1 (PD-1) and PD-ligand 1 (PD-L1) expression in cancer cells and tumor-infiltrating lymphocytes in ovarian high grade serous carcinoma. *Oncotarget* **2016**;7:1486-99.
45. Schalper KA, Velcheti V, Carvajal D, Wimberly H, Brown J, Pusztai L*, et al.* In situ tumor PD-L1 mRNA expression is associated with increased TILs and better outcome in breast carcinomas. *Clin Cancer Res* **2014**;20:2773-82.

46. Herbst RS, Soria JC, Kowanetz M, Fine GD, Hamid O, Gordon MS*, et al.* Predictive correlates of response to the anti-PD-L1 antibody MPDL3280A in cancer patients. *Nature* **2014**;515:563-7.

47. Mace TA, Shakya R, Pitarresi JR, Swanson B, McQuinn CW, Loftus S*, et al.* IL-6 and PD-L1 antibody blockade combination therapy reduces tumour progression in murine models of pancreatic cancer. *Gut* **2018**;67:320-32.

48. Dijkgraaf EM, Santegoets SJ, Reyners AK, Goedemans R, Wouters MC, Kenter GG*, et al.* A phase I trial combining carboplatin/doxorubicin with tocilizumab, an anti-IL-6R monoclonal antibody, and interferon-alpha2b in patients with recurrent epithelial ovarian cancer. *Ann Oncol* **2015**;26:2141-9.

Figure legends

Figure 1. *In vivo* reduction of metastatic colonization of colon cancer cells in the livers of *Il6*$^{-/-}$ mice. GFP-transfected CT26 murine colon cancer cells (2×10^5) were intrasplenically inoculated into wild-type (*Il6*$^{+/+}$) and *Il6*$^{-/-}$ BALB/c mice (day 0). **A,** Experimental scheme is shown. **B,** Sera were collected from normal and liver metastatic colonization model mice. Serum IL-6 levels (n = 9–10, cumulative results from three independent experiments) are shown. **C** and **D,** Serum AST and ALT levels in liver metastatic colonization model mice (n = 7, cumulative results from two independent experiments) and liver and total body weights (n = 4, two independent experiments) were measured. Percentages of liver weight per total body weight were calculated**. E,** HE staining of liver tissues was performed. **G,** Metastatic colonization in liver tissue was evaluated using an *in vivo* imaging system at day 14. Representative images of normal liver and GFP-expressing CT26 cell-bearing livers are shown. **H,** Photon flux ratios were determined from images of liver metastatic colonization model mice (n = 4, three independent experiments). **I,** The survival rate of liver metastatic colonization model mice was monitored for 60 days and the percentage survival rate (n = 11, two independent experiments) is shown. **J,** CT26-*Il6*KO cells (2×10^5) were intrasplenically inoculated into *Il6*$^{+/+}$ or *Il6*$^{-/-}$ BALB/c mice (day 0). HE staining of liver tissue was performed at 21 days after inoculation (two independent experiments).

Representative micrographs are shown. Bars in the images represent 500 μm (**E** and **J**). Ratios of tumor area relative to total liver tissue area were calculated by ImageJ software (**F** and **K**). Means and SDs of the data from four independent mice are shown (**F, H,** and **K)**. *P < 0.05 by Dunnett's test (**B**), Student's t-test (**C, D, F, H** and **K**) and log-rank test (**I**).

Figure 2. Accumulation of mature DCs and effector memory-type CD8$^+$ T cells in liver metastases of *Il6*$^{-/-}$ mice. GFP-transfected CT26 murine colon cancer cells (2×10^5) were intrasplenically inoculated into *Il6*$^{+/+}$ or *Il6*$^{-/-}$ mice (day 0). **A,** IHC staining of liver tissue was performed to evaluate CD11c and CD3 levels at day 14. Representative micrographs are shown. Bars represent 200 μm. **B,** Whole cells were collected from liver tissues of CT26 tumor-bearing *Il6*$^{+/+}$ or *Il6*$^{-/-}$ mice at day 14. Surface expression levels of CD11c, I-Ad, CD44, CD62L, and CD8 on 7-AAD$^-$CD45$^+$ cells were evaluated by flow cytometry. The representative data for CD11c^{high}I-Ad^{high} DCs and CD44$^+$CD62L$^-$CD8$^+$ T cells are shown in the figures. Percentages of CD11c^{high}I-Ad^{high} cells and CD44$^+$CD62L$^-$CD8$^+$ cells relative to total CD45$^+$ cells were calculated and the means and SDs (n = 3–4, three independent experiments) are indicated. *P < 0.05 by Student's t-test. **C,** Relative expression of *Il12a*, *Il12b*, *Ifna*, *Ifnb*, *Arg1*, and *Il10* relative to *Actb* in CD11c$^+$ DCs from liver tissues were evaluated and the means and SDs (n =

3–10, two to three independent experiments) are shown. *$P < 0.05$ by Student's t-test. **D,** Percentage cytotoxicity of immune cells obtained from tumor-bearing liver tissues against CT26 cells as evaluated by flow cytometry. Means and SDs (n = 4, three independent experiments) are shown. *$P < 0.05$ vs. *Il6*$^{+/+}$. **E,** Perforin and granzyme B levels in CD8$^+$ T cells from liver tissues were determined by flow cytometry at day 14. ΔMFIs of perforin and granzyme B relative to each isotype control are shown. Means and SDs (n = 5–7, cumulative results from three independent experiments) are shown. *$P < 0.05$ by Student's t-test.

Figure 3. IL-12 and CD8$^+$ effector T cells reduce metastatic colonization in the livers of *Il6*$^{-/-}$ mice. GFP-transfected CT26 cells (2×10^5) were intrasplenically inoculated into control liposome-, clodronate liposome-, control IgG-, anti-CD8 mAb, or anti-IL-12 mAb-treated *Il6*$^{-/-}$ mice (day 0). **A, D**, and **G,** HE staining of liver tissue was performed at 14 days after inoculation. Representative micrographs are shown. Bars represent 500 μm. **B, E**, and **H**, Metastatic colonization of GFP-expressing CT26 cells in the liver were evaluated by an *in vivo* imaging system at day 14. Representative images are shown. **C, F**, and **I,** Photon flux ratios were evaluated from the images (n = 4–6, three independent experiments) and the means and SDs are shown. *$P < 0.05$ by Student's t-test. **J,** IHC was performed to evaluate CD11c and CD3 levels at day 14.

Representative micrographs are shown. Bars represent 200 μm. **K,** Whole cells were collected from liver tissues of control IgG- or anti-IL-12-mAb-treated CT26 tumor-bearing *Il6*$^{-/-}$ mice at day 14. Surface expression levels of CD11c, I-Ad, CD44, CD62L, and CD8 on 7-AAD^{-}CD45^{+} cells were evaluated by flow cytometry. The representative data for CD11c^{high}I-Ad^{high} DCs and CD44^{+}CD62L^{-}CD8^{+} T cells are shown in the figures. Percentages of CD11c^{high}I-Ad^{high} cells and CD44^{+}CD62L^{-}CD8^{+} cells relative to total CD45^{+} cells were calculated and the means and SDs (n = 4, two independent experiments) are indicated. *P < 0.05 by Student's t-test. **L,** Percentage cytotoxicity of immune cells obtained from liver tissues against CT26 cells was evaluated by flow cytometry. Means and SDs (n = 3, two independent experiments) are shown. *P < 0.05 vs. corresponding control IgG group by Student's t-test. **M,** Perforin and granzyme B levels in CD8^{+} T cells from the liver were determined by flow cytometry at day 14. ΔMFIs against each isotype control were calculated. Means and SDs (n = 3, two independent experiments) are shown. *P < 0.05 by Student's t-test.

Figure 4. Upregulation of interferon α/β-STAT1 signaling and induction of PD-L1 expression on colon cancer cells in tumor-bearing *Il6*$^{-/-}$ mice. GFP-transfected CT26 cells were intrasplenically inoculated into control IgG- or anti-IFN-AR1 mAb-treated *Il6*$^{-/-}$ mice (day 0). **A,** HE staining of the liver was performed at 14 days after

inoculation. Representative micrographs are indicated. Bars represent 500 μm. **B,** Metastatic colonization of GFP-expressing CT26 cells in the liver was evaluated by an *in vivo* imaging system at day 14. **C,** Photon influx ratios were calculated (n = 4, three independent experiments). *P < 0.05 by Student's t-test. **D** and **E,** CT26 cells were stimulated with IFN-α and IFN-β in the presence or absence of a STAT1 inhibitor for 24 h *in vitro*. Surface levels of H-2K^{d} and PD-L1 on CT26 cells were evaluated by flow cytometry. Representative data are shown. ΔMFIs against isotype controls were calculated (n = 3, three independent experiments). *P < 0.05 by Dunnett's test. **F,** IHC staining of the liver was performed to evaluate phospho (Tyr701)-STAT1. Representative micrographs are shown. Bars represent 200 μm. **G,** Phospho-STAT1 expression levels on GFP^{+}CD45^{-} CT26 cells were determined by flow cytometry at day 14. ΔMFIs of phospho-STAT1 expression against each isotype control were calculated (n = 3–5, two independent experiments). *P < 0.05 by Student's t-test. **H,** Surface levels of H-2K^{d} and PD-L1 on GFP^{+}CD45^{-} CT26 cells obtained from livers at day 14 were evaluated by flow cytometry. Representative data are shown. ΔMFIs were calculated (n = 3–4, three independent experiments). *P < 0.05 by Student's t-test. Means and SDs are shown (**C**–**E, G**, and **H**).

Figure 5. Augmentation of the anti-tumor effect of PD-L1 blockade on metastatic

colonization in the livers of *Il6*$^{-/-}$ mice. GFP-transfected CT26 cells were intrasplenically inoculated into *Il6*$^{-/-}$ mice (day 0). Control IgG or anti-PD-L1 mAb were injected intraperitoneally into *Il6*$^{-/-}$ mice at day 5 and then every 4 days thereafter. **A,** HE staining of liver tissue was performed at 19 days after inoculation. Representative micrographs are indicated. Bars represent 500 μm. **B,** Metastatic colonization at day 19 was evaluated with an *in vivo* imaging system. **C,** Photon flux ratios were evaluated (n = 3–4, two independent experiments). **P* < 0.05 by Student's t-test. **D,** IHC staining of liver tissue was performed for CD11c and CD3. Representative micrographs are shown. Bars represent 200 μm. **E,** Whole cells were collected from liver tissues of control IgG- or anti-PD-L1-mAb-treated CT26 tumor-bearing *Il6*$^{-/-}$ mice at day 14. Surface expression levels of CD11c, I-Ad, CD44, CD62L, and CD8 on 7-AAD^{-}CD45^{+} cells were evaluated by flow cytometry. The representative data for CD11c^{high}I-Ad^{high} DCs and CD44^{+}CD62L^{-}CD8^{+} T cells are shown in the figures. Percentages of CD11c^{high}I-Ad^{high} cells and CD44^{+}CD62L^{-}CD8^{+} cells relative to total CD45^{+} cells were calculated and the means and SDs (n = 4, two independent experiments) are indicated. **P* < 0.05 by Student's *t*-test. **F,** Percentage cytotoxicity of immune cells from the liver against CT26 cells was evaluated by flow cytometry (n = 3, two independent experiments). **P* < 0.05 vs. control IgG group. **G,** Perforin and granzyme B levels in CD8^{+} T cells from the liver were determined by flow cytometry and the ΔMFIs were

calculated (n = 3, two independent experiments). *$P < 0.05$ by Student's t-test. **H,** The survival rate of mice (n = 24, two independent experiments) was monitored for 40 days and the percentage survival is shown. *P value was determined by the log-rank test. **I,** Proposed model of the present study. Mean and SDs are shown **(C** and **E**–**G)**.

Figure 6. Correlation between IL-6 expression in primary tumor tissues and DFS of PD-L1-negative and PD-L1-positive CRC patients. IHC of primary tumor tissues of CRC patients (n = 108) was conducted to evaluate IL-6 and PD-L1 levels using anti-IL-6 and anti-PD-L1 antibodies, respectively. **A,** Representative micrographs of tumor tissues from IL-6-positive and -negative and PD-L1-positive and -negative patients are shown. Bars in the images represent 100 μm. **B,** Kaplan-Meier estimates of DFS for 108 CRC patients stratified into two groups: IL-6-negative (55 patients) or IL-6-positive (53 patients) and PD-L1-negative (71 patients) or PD-L1-positive (37 patients). **C,** Kaplan-Meier estimates of DFS for 71 PD-L1-negative CRC patients stratified into two groups: IL-6-negative (32 patients) or IL-6-positive (39 patients). Kaplan-Meier estimates of DFS for 37 PD-L1-positive CRC patients stratified into two groups: IL-6-negative (23 patients) or IL-6-positive (14 patients).

Figure 1. Toyoshima et al.

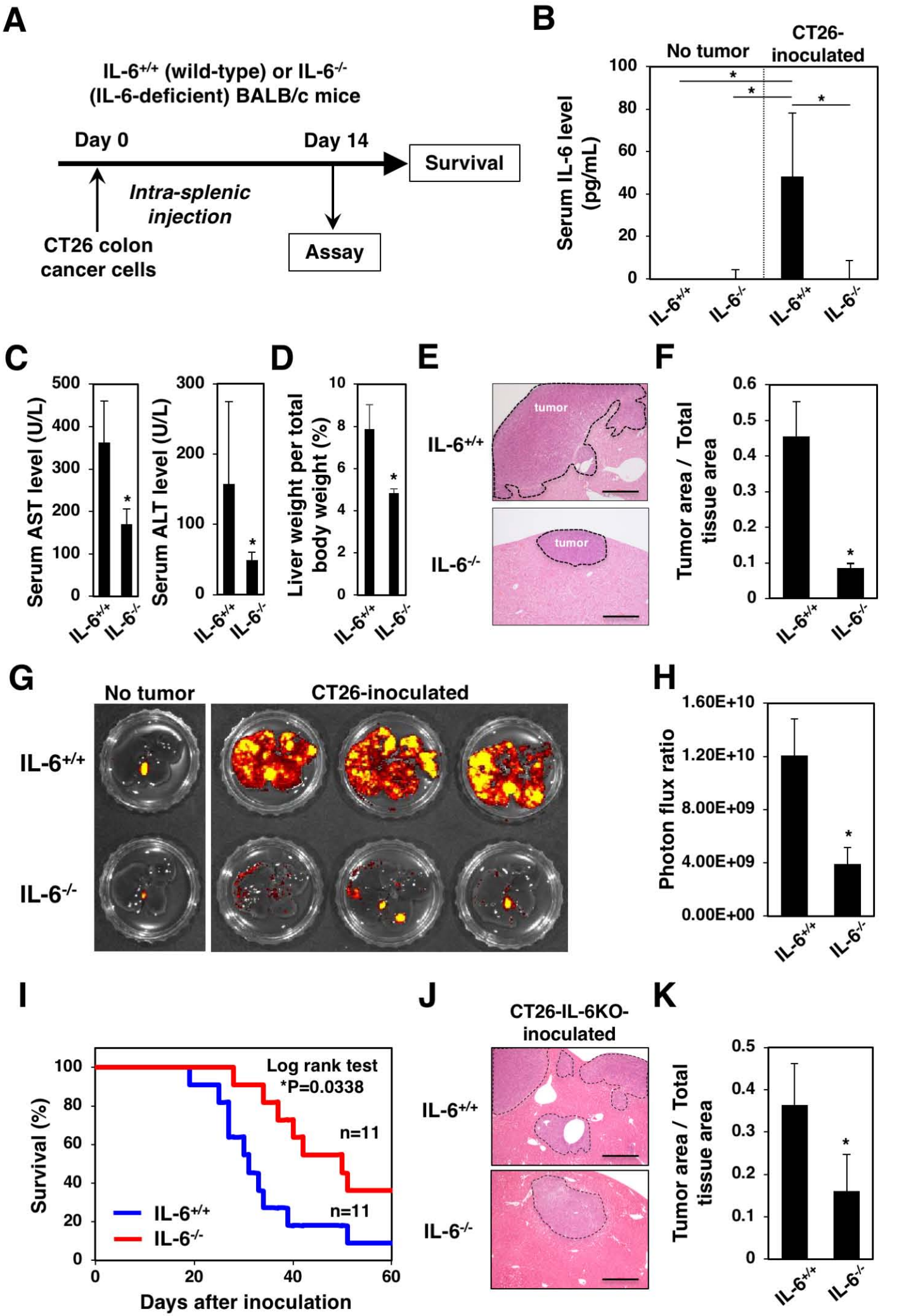

Figure 2. Toyoshima et al.

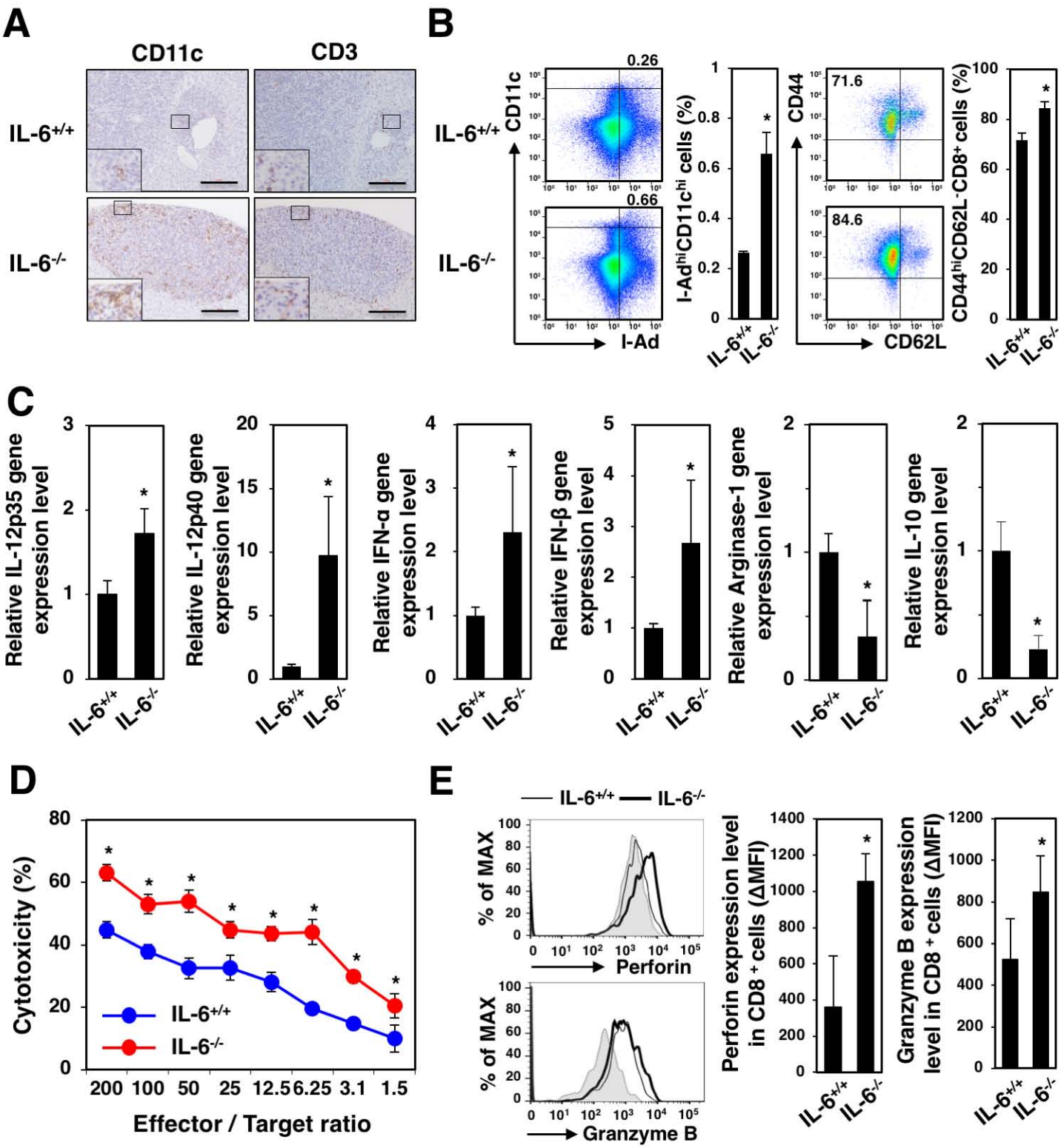

Figure 3. Toyoshima et al.

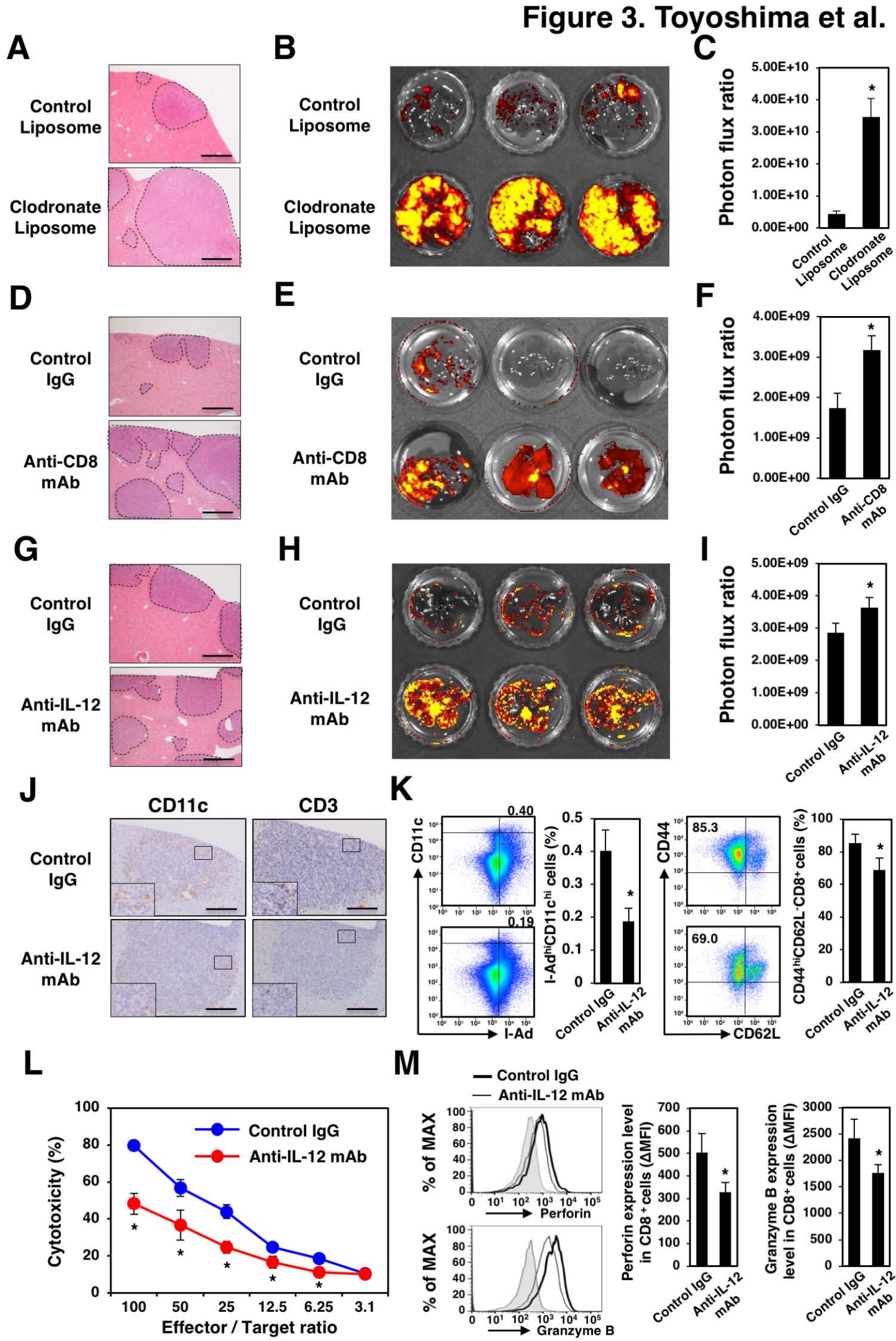

Figure 4. Toyoshima et al.

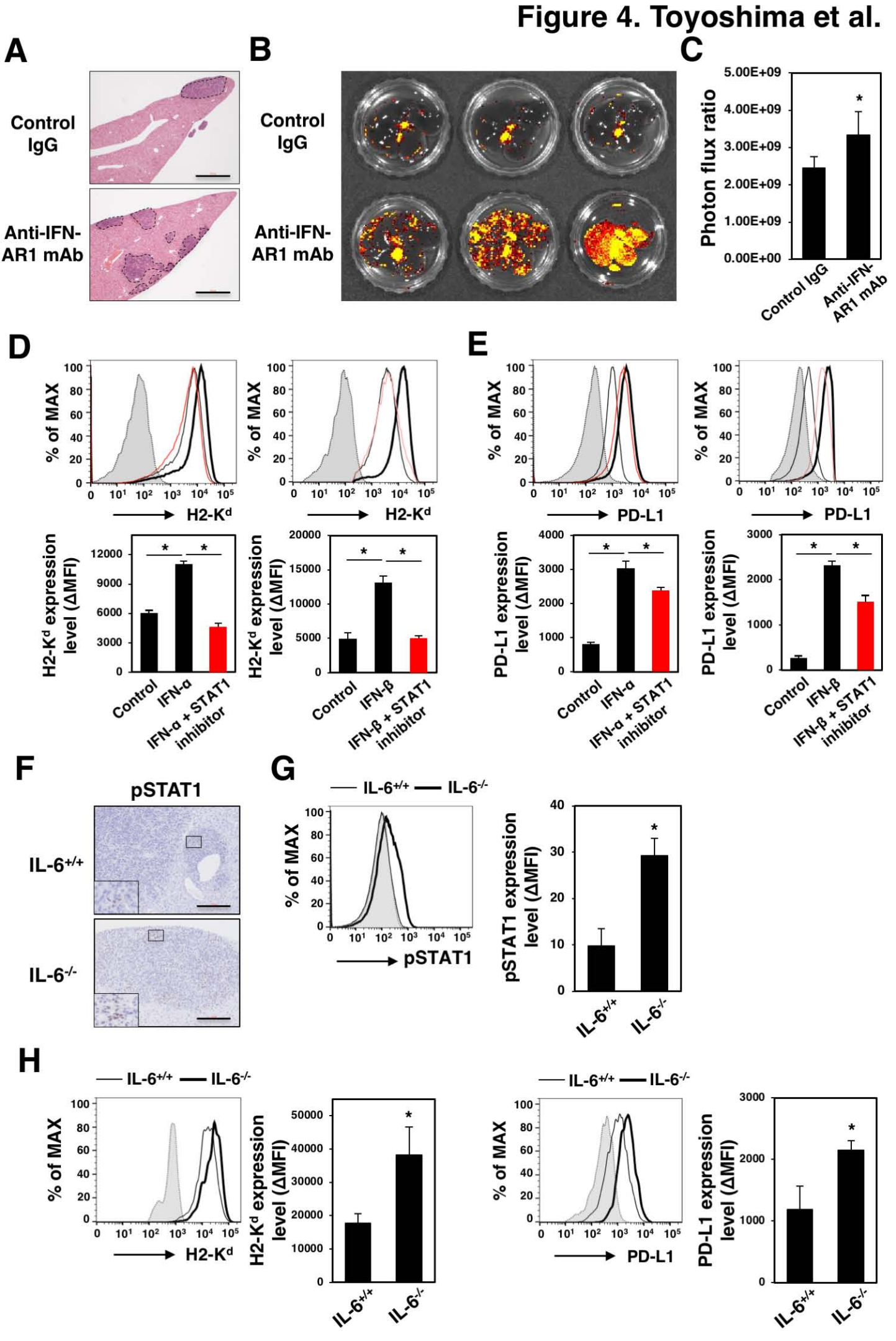

Figure 5. Toyoshima et al.

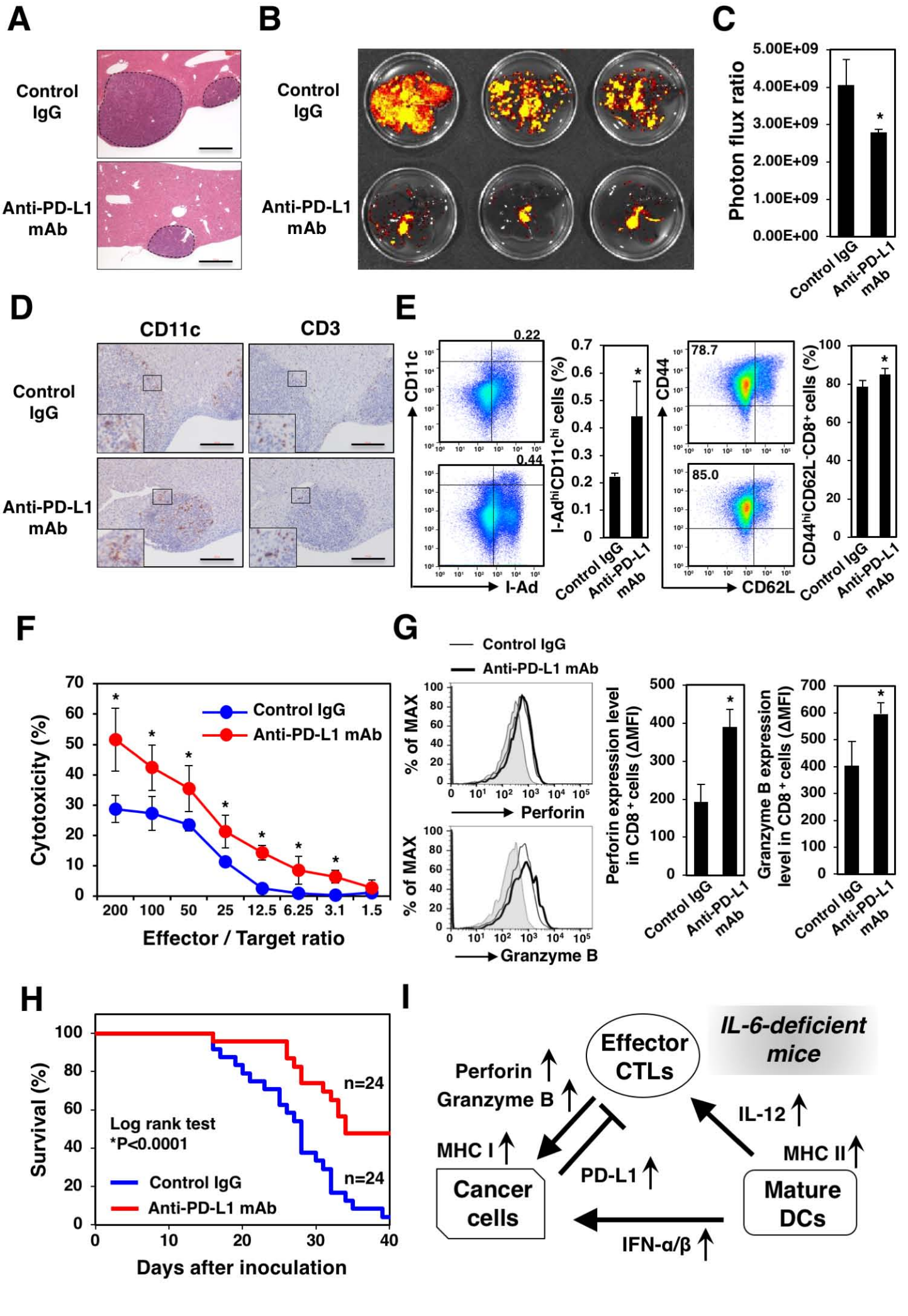

Figure 6. Toyoshima et al.